

Rethinking Epistemic and Aleatoric Uncertainty for Active Open-Set Annotation: An Energy-Based Approach

Chen-Chen Zong, Sheng-Jun Huang*
Nanjing University of Aeronautics and Astronautics
Nanjing, 211106, China
{chencz, huangsj}@nuaa.edu.cn

Abstract

Active learning (AL), which iteratively queries the most informative examples from a large pool of unlabeled candidates for model training, faces significant challenges in the presence of open-set classes. Existing methods either prioritize query examples likely to belong to known classes, indicating low epistemic uncertainty (EU), or focus on querying those with highly uncertain predictions, reflecting high aleatoric uncertainty (AU). However, they both yield suboptimal performance, as low EU corresponds to limited useful information, and closed-set AU metrics for unknown class examples are less meaningful. In this paper, we propose an Energy-based Active Open-set Annotation (EAOA) framework, which effectively integrates EU and AU to achieve superior performance. EAOA features a $(C + 1)$ -class detector and a target classifier, incorporating an energy-based EU measure and a margin-based energy loss designed for the detector, alongside an energy-based AU measure for the target classifier. Another crucial component is the target-driven adaptive sampling strategy. It first forms a smaller candidate set with low EU scores to ensure closed-set properties, making AU metrics meaningful. Subsequently, examples with high AU scores are queried to form the final query set, with the candidate set size adjusted adaptively. Extensive experiments show that EAOA achieves state-of-the-art performance while maintaining high query precision and low training overhead. The code is available at this [link](#).

1. Introduction

The success of deep neural networks (DNNs) is largely fueled by large-scale, accurately labeled datasets [16, 49]. However, acquiring such data is often expensive and time-consuming primarily due to the labor-intensive nature of manual labeling [30, 50]. To save labeling costs, recent research has focused on developing effective model training

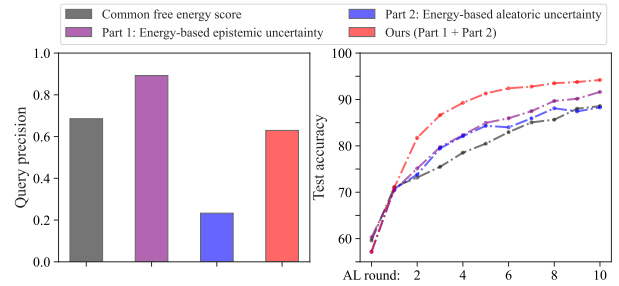


Figure 1. Dataset: CIFAR-10; mismatch ratio: 40%. Our motivation: in open-set scenarios, querying examples with low epistemic uncertainty yields high query precision, but the overall information content is low, resulting in poor model performance. Focusing on examples with high aleatoric uncertainty also leads to poor performance, as the model’s assessment of this uncertainty becomes meaningless for open-set examples. Nevertheless, an effective combination of the two can lead to a superior outcome.

techniques that leverage limited and insufficiently labeled data [30, 37, 46]. Among them, active learning (AL) has emerged as a popular framework, which iteratively selects the most informative examples from the unlabeled data pool and queries their labels from the Oracle [12, 30, 34].

Existing AL methods can be categorized into three types based on their sampling strategies: uncertainty-based [2, 10, 42, 50], diversity-based [25, 33, 40], and hybrid strategies [1, 11, 31]. Most of these methods operate under the closed set assumption, which posits that the classes in the unlabeled data match those in the labeled data. However, in real-world scenarios, it is challenging and often costly to ensure that no open-set classes are present in the unlabeled data. Meanwhile, several studies [6, 26, 28, 31] have shown that these methods perform poorly when open-set classes are involved, as such examples tend to receive uncertain model predictions and exhibit distinct features. Therefore, developing effective AL methods for open-world scenarios, where open-set classes exist, is of significant importance.

Recently, this emerging research problem has garnered

*Corresponding Author

considerable attention [6, 26, 28, 31, 50]. For instance, in LfOSA [26], the authors formulate this problem as open-set annotation (OSA) and utilize queried unknown class examples to train a $(C + 1)$ -class detector for rejecting open-set examples and focusing more on selecting known class ones. Two recent methods, EOAL [31] and BUAL [50], adopt a structure similar to LfOSA, with EOAL aimed at improving the recognition of known class examples, while BUAL focuses more on sampling highly uncertain examples. Despite demonstrating high query precision, our findings reveal that these methods can not achieve satisfactory test accuracy and struggle to identify the most informative examples.

To analyze the reasons behind their failure, we review the concept of uncertainty quantification¹. Epistemic uncertainty refers to a measure that remains high for instances not previously encountered and decreases when these instances are included in the training [14, 35]. In contrast, aleatoric uncertainty is characterized by elevated values in ambiguous examples [14, 35]. In closed-set settings, examples with high epistemic uncertainty tend to reside in low-density regions of the representation space, while those with high aleatoric uncertainty may appear around the decision boundary due to ambiguous features. Both types are potential targets for our queries. However, in open-set scenarios, examples with high epistemic uncertainty are likely to be open-set instances, and aleatoric uncertainty is meaningful only in closed-set contexts, as it reflects the ambiguity between different observable classes² [14, 22]. Therefore, selecting examples with low epistemic uncertainty (to ensure a closed set) and high aleatoric uncertainty is a more reasonable choice. However, LfOSA and EOAL focus on querying examples with low epistemic uncertainty, while BUAL prioritizes querying those with high aleatoric uncertainty. This may be the potential reason for their failure.

To validate this, we present the results in Figure 1. As shown, focusing solely on either epistemic or aleatoric uncertainty in an open-world scenario results in suboptimal performance. However, effectively combining both leads to a significant improvement. Inspired by this, we propose **Energy-based Active Open-set Annotation (EAOA)**, an approach that effectively queries the most informative examples by considering both types of uncertainty. EAOA maintains two networks: a $(C + 1)$ -class detector and a C -class target classifier, with the following contributions:

- An energy-based epistemic uncertainty measure is designed for the detector, expressed as the free energy score on known classes minus that on the unknown class. This measure integrates both learning-based and data-driven perspectives, enabling reliable uncertainty assessment in data-limited scenarios.

- An energy-based aleatoric uncertainty measure is proposed for the target classifier, defined as the free energy score on all classes minus that on secondary classes.
- A coarse-to-fine querying strategy is proposed. It first selects examples with low epistemic uncertainty to form a smaller candidate set, ensuring closed-set properties, which makes aleatoric uncertainty meaningful. Then, it queries examples with high aleatoric uncertainty within this set, with the candidate set size adaptively adjusted through a novel target-driven strategy.
- A margin-based energy loss is introduced for the detector training, aimed at maximizing the free energy score on known classes while minimizing that on the unknown class, thereby enhancing the unknown class detection.
- Extensive experiments show that EAOA outperforms current state-of-the-art methods in test accuracy, query precision, and training efficiency.

2. Related Work

Active learning (AL) has garnered great research interest as a primary framework for reducing labeling costs by querying the most informative examples for model training. AL’s query methods can be categorized based on their data sources into three types: query-synthesizing [19, 20, 47], stream-based [7, 23], and pool-based approaches [2, 6, 10, 12, 50]. Among these, pool-based methods are currently the mainstream, operating under the assumption of a large pool of available unlabeled data, from which a subset of examples is selected for annotation in each AL round. These query methods can be further divided into three categories: 1) uncertainty-based strategies [2, 10, 17, 42], which select instances for which labeling is least certain; 2) diversity-based strategies [25, 33, 40], which query instances that are most representative or exhibit the greatest feature diversity; and 3) hybrid strategies [1, 11, 31], which combine both to achieve better performance.

Open-set recognition (OSR) refers to a system’s ability to differentiate between data types it has encountered during training (in-distribution (ID) data) and those it has not previously seen (out-of-distribution (OOD) data). Earlier studies employed traditional machine learning techniques such as support vector machines [13, 32], extreme value theory (EVT) [43], nearest class mean classifier [3], and nearest neighbor [21]. Recently, there has been growing interest in using generative models to learn representation spaces focused exclusively on known examples [27, 29, 36, 44]. Other techniques often aim to simulate unknown examples, providing a more intuitive approach to OSR [4, 5, 8, 24, 45]. However, simply applying these methods in AL scenarios under the open-world assumption often leads to failure for two main reasons. First, the recognition performance of these methods heavily relies on the classifier’s effectiveness; when the classifier underperforms—a common occur-

¹ A detailed introduction with intuitive illustrations is in Appendix A.

² Essentially, the class probability $p(y|x) = \frac{p(x,y)}{p(x)}$ is meaningful only when $p(x) \neq 0$, i.e., x must be an observing example from a known class.

rence in AL scenarios—the overall performance can decline significantly [38]. Second, some genuine unknown class examples are inevitably labeled during the labeling process, and OSR methods may not effectively utilize them.

Active open-set annotation (AOSA) refers to AL tasks under open-world scenarios, which aligns more closely with practical application scenarios and has become a research hotspot in recent years [6, 26, 28, 31, 50]. CCAL [6] and MQNet [28] employ contrastive learning and established metrics respectively to assess sample purity and informativeness, utilizing heuristic and meta-learning approaches, respectively, to achieve a balance. However, by not fully leveraging labeled unknown class examples, they provide inadequate assessments, leading to poorer model performance. LfOSA [26] incorporates labeled unknown class examples to train an additional $(C + 1)$ -class classifier (a.k.a, detector), using the maximum activation values (MAVs) to identify known class examples. EOAL [31] enhances the detector by adding an additional binary classifier head and uses entropy values, calculated separately for known and unknown classes, to identify known class examples. BUAL [50] defines positive uncertainty and negative uncertainty respectively, and utilizes the detector’s OOD probabilities to balance, aiming to identify highly uncertain examples. However, as previously noted, these methods fail to select examples with both low epistemic uncertainty and high aleatoric uncertainty, resulting in suboptimal performance.

3. Methodology

3.1. Preliminaries

Notations. Consider the problem of ordinary C -class classification. In active open-set annotation (AOSA) tasks, we start with a limited labeled dataset $\mathcal{D}_L^{kno} = \{(x_i^L, y_i^L)\}_{i=1}^{\mathcal{N}_L}$ containing \mathcal{N}_L examples from known classes for training, alongside a sufficiently large unlabeled data pool $\mathcal{D}_U = \{x_i^U\}_{i=1}^{\mathcal{N}_U}$ consisting of \mathcal{N}_U examples from both known and unknown classes for querying. The label y_i^L of an instance x_i^L belongs to $\{1, \dots, C\}$, whereas the label y_i^U of an instance x_i^U is not provided prior to Oracle labeling and falls within $\{1, \dots, C + 1\}$, with $C + 1$ representing all unknown classes. At each active learning (AL) cycle, a batch of b examples, denoted as $X^{query} = X_{kno}^{query} \cup X_{unk}^{query}$, is selected according to a specified query strategy and sent to Oracle for labeling. Then, \mathcal{D}_L^{kno} and \mathcal{D}_U are updated accordingly, and X_{unk}^{query} forms the unknown class dataset \mathcal{D}_L^{unk} with $\mathcal{D}_L = \mathcal{D}_L^{kno} \cup \mathcal{D}_L^{unk}$.

Overview. As outlined in the Introduction, addressing the AOSA problem requires first ensuring that the queried examples exhibit low epistemic uncertainty to approximate a closed set, enabling meaningful aleatoric uncertainty assessment, and then querying examples with high aleatoric uncertainty. To achieve this goal, we propose an Energy-

based Active Open-set Annotation (EAOA) framework, as illustrated in Figure 2, which primarily consists of three key components: active sampling, detector training, and classifier training. Specifically, we begin by training a detector network to evaluate the epistemic uncertainty of examples from both learning-based and data-driven perspectives, leveraging the labeled data from both known and unknown classes. Next, we assess the aleatoric uncertainty of examples by utilizing the free energy discrepancy in predictions made by the target classifier. Finally, we query a smaller candidate set of examples with low epistemic uncertainty first, with the set dynamically adjusting by rounds, and then acquire the query set with high aleatoric uncertainty.

3.2. Energy-based Epistemic and Aleatoric Uncertainty for Active Sampling

Energy-based epistemic uncertainty. Energy-based models (EBMs) [18, 39] build a function $E(x) : \mathbb{R}^D \rightarrow \mathbb{R}$ to map a D -dim data point to a scalar and defines the probability distribution in multi-class settings through logits as:

$$p(y|x) = \frac{e^{-E(x,y)}}{\int_y e^{-E(x,y)}} = \frac{e^{f_y(x)}}{\sum_{c=1}^C e^{f_c(x)}} = \frac{e^{-E(x,y)}}{e^{-E(x)}}, \quad (1)$$

where $f_y(x)$ denotes the predicted logit of model f for instance x regarding label y , $E(x, y) = -f_y(x)$, and $E(x) = -\log \sum_{c=1}^C e^{-E(x,c)}$ is called free energy. The probability density of x in an EBM can be written as:

$$p(x) = \frac{e^{-E(x)}}{\int_x e^{-E(x)}} = \frac{\int_y e^{-E(x,y)}}{\int_x \int_y e^{-E(x,y)}} = \frac{e^{-E(x)}}{\mathcal{Z}}. \quad (2)$$

This implies that for two data points, x_1 and x_2 , if $E(x_1) > E(x_2)$, then x_1 lies in a sparser region compared to x_2 w.r.t. the marginal distribution. This aligns with epistemic uncertainty: high-uncertainty examples are distributed in low-density regions due to their lower occurrence frequency.

Nevertheless, free energy is not ideal for directly measuring epistemic uncertainty in the AOSA task, as the underlying EBM does not fully utilize the information contained in the labeled unknown class examples. To counter this, we group all unknown classes into the $C + 1$ category, train a multi-class classifier (i.e., the detector), and extend the free energy theory by making the following Remark 1.

Remark 1 For AOSA tasks, the epistemic uncertainty (EU) of x can be expressed through the free energy score on known classes minus that on the unknown class³,

$$\begin{aligned} EU(x) &= E_{kno}(x) - E_{unk}(x) \\ &= -\log \sum_{c=1}^C e^{-E(x,c)} + \log \left(1 + e^{-E(x,C+1)} \right). \end{aligned} \quad (3)$$

³ $E_{unk}(x)$ is determined by label-wise free energy (see Appendix B).

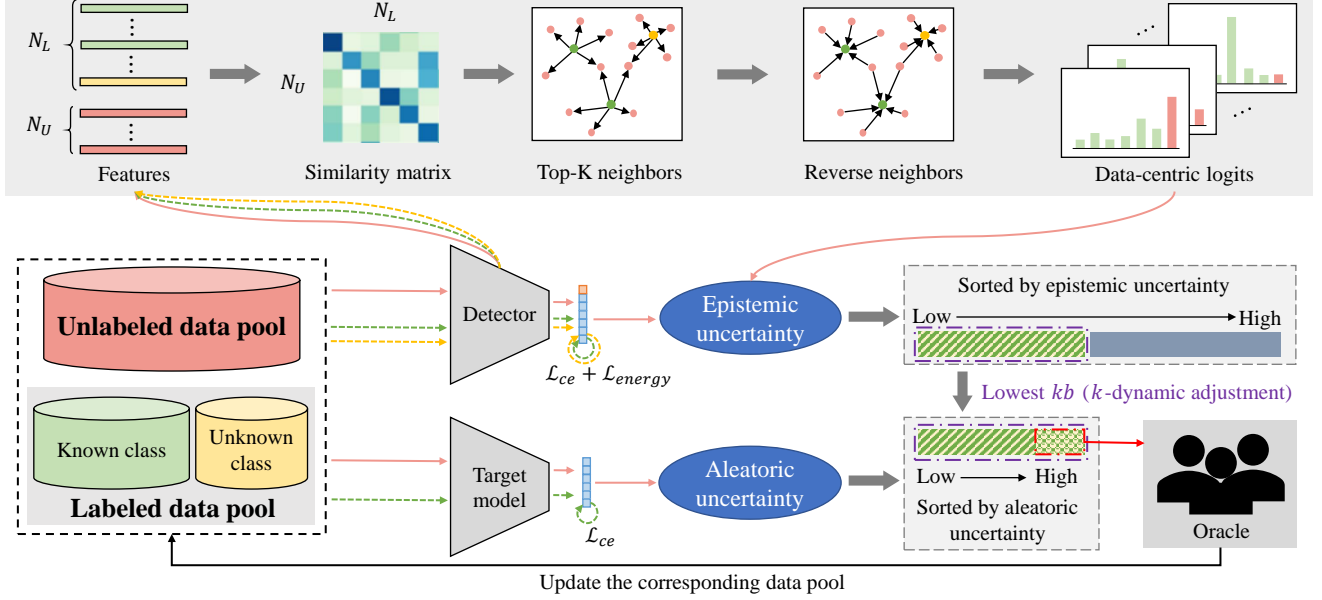


Figure 2. The framework of EAOA. It consists of three general steps: model training, example selection, and Oracle labeling. In the model training phase, a detector is trained to assess epistemic uncertainty (EU) from both learning-based and data-driven perspectives, along with a target classifier to evaluate aleatoric uncertainty (AU) based on class confusion. In the example selection phase, kb examples with the lowest EU scores are chosen first, followed by querying b examples with the highest AU scores, where k is adaptively adjusted based on the target precision. In the Oracle labeling phase, the queried examples are assigned labels, and all relevant data pools are updated accordingly.

As such, for two given data points x_1 and x_2 , the inequality $EU(x_1) > EU(x_2)$ implies that x_1 is occurring from a denser region w.r.t. the unknown class compared to x_2 .

Since labeled data in AL is often quite limited, relying solely on the detector’s predictions to assess the epistemic uncertainty of examples may not be sufficiently reliable. To obtain a more reliable measurement, we evaluate the epistemic uncertainty of examples in two ways: 1) a learning-based perspective that directly uses the detector’s predictions, and 2) a data-driven perspective that relies on the similarity to labeled examples from different classes. To this end, we utilize the detector to extract features and emit K arrows from each instance in the labeled data pool \mathcal{D}_L to its K nearest neighbors in the unlabeled data pool \mathcal{D}_U based on cosine distance. For a data point x_i^U , its probability given class y can be approximated as:

$$p(x_i^U|y) = \frac{\# \text{ of Arrows}_{(x_j^L, y)}}{|X^y|} \quad (4)$$

where $\# \text{ of Arrows}_{(x_j^L, y)}$ denotes the total number of arrows directed at x_i^U from examples with label y , and $|X^y|$ represents the total number of examples with label y in \mathcal{D}_L . If x_i^U is in a region where examples with label y densely exist, it is likely to receive more arrows, and vice versa.

Then, by virtue of Bayes’ theorem, we define the data-

centric class probability distribution of x_i^U as

$$p(y|x_i^U) = \frac{p(x_i^U|y)p(y)}{\sum_{c=1}^{C+1} p(x_i^U|c)p(c)}. \quad (5)$$

Here, the prior $p(y)$ is the probability of observing class y , and can be approximately determined by the sample count for each class in \mathcal{D}_L :

$$p(y) = \frac{|X^y|}{\sum_{c=1}^{C+1} |X^c|}. \quad (6)$$

Based on Eqs. (1), (4), (5), and (6), we can obtain:

$$p(y|x_i^U) = \frac{\# \text{ of Arrows}_{(x_j^L, y)}}{\sum_{c=1}^{C+1} \# \text{ of Arrows}_{(x_j^L, c)}} = \frac{e^{-E(x_i^U, y)}}{e^{-E(x_i^U)}}. \quad (7)$$

As such, we can define the specific form of the energy function from a data-driven perspective to calculate the epistemic uncertainty of examples, as stated in Remark 1.

Here, for a given data point x_i^U , the uncertainty scores calculated in two different ways are denoted as $EU_L(x_i^U)$ and $EU_D(x_i^U)$. We first gather the uncertainty scores for all examples in \mathcal{D}_U to form sets $\{EU_L(x_1^U), \dots, EU_L(x_{N_U}^U)\}$ and $\{EU_D(x_1^U), \dots, EU_D(x_{N_U}^U)\}$, and then fit two two-component Gaussian Mixture Models (GMMs) respectively to convert these scores into a probabilistic format. Suppose a tilde is added to denote the probabilistic format, we apply

an element-wise product rule to obtain the final epistemic uncertainty score of x_i^U :

$$\tilde{EU}(x_i^U) = \tilde{EU}_L(x_i^U) \odot \tilde{EU}_D(x_i^U). \quad (8)$$

Energy-based aleatoric uncertainty. Aleatoric uncertainty arises through inherent noise in the data, that is, for the same instance x , different labels might be observed if multiple annotators label it independently. This means that aleatoric uncertainty can be defined based on the confusion between classes. As such, we further extend the free energy theory by making the following Remark 2.

Remark 2 For AL tasks, the aleatoric uncertainty (AU) of x can be expressed through the free energy scores on all classes minus that on secondary classes,

$$\begin{aligned} AU(x) &= E(x) - E_{\text{secondary classes}}(x) \\ &= -\log \sum_{c=1}^C e^{-E(x,c)} + \log \left[\sum_{c=1}^C e^{-E(x,c)} - e^{-E(x,y_{\max})} \right], \end{aligned} \quad (9)$$

where y_{\max} is the most probable label for x . This implies that for two data points x_1 and x_2 , if inequality $AU(x_1) > AU(x_2)$ holds, then x_1 occurs in a region closer to the decision boundary compared to x_2 .

Similarly, we gather the uncertainty scores for all examples in \mathcal{D}_U to form set $\{AU(x_1^U), \dots, AU(x_{N_U}^U)\}$, and then fit a two-component GMM to convert these scores into a probabilistic format, i.e., $\{\tilde{AU}(x_1^U), \dots, \tilde{AU}(x_{N_U}^U)\}$.

Target-driven adaptive active sampling. After having epistemic uncertainty scores and aleatoric uncertainty scores, we form the query set based on the strategy outlined in Figure 2. Specifically, in each active sampling round, we perform the querying in two rounds. In the first round, kb examples with the lowest epistemic uncertainty scores are selected. Then, according to aleatoric uncertainty, we choose the top b examples with the highest scores from the candidates obtained in the first round to query their labels.

Obviously, the choice of the k value is critical. If k is too small, such as $k = 1$, it maximizes the likelihood that the queried examples belong to the closed-set classes. However, since the candidate set size matches the query set size, aleatoric uncertainty cannot effectively contribute. On the contrary, if the k value is too large, the closed-set condition of the candidate set cannot be ensured, rendering aleatoric uncertainty meaningless. Meanwhile, the optimal k value often varies for different datasets. To enhance the strategy’s generalizability, we introduce the expected target precision for known class queries to drive the adaptive adjustment of the k value. The relation between the two is as follows:

$$k_{t+1} = \begin{cases} k_t + a & \text{if } rP - tP > z, \\ k_t - a & \text{if } tP - rP > z, \\ k_t & \text{if } |tP - rP| \leq z, \end{cases} \quad (10)$$

where k_t is the value of k in the t -th AL round, tP is the expected target precision, rP is the real query precision calculated as $rP = \frac{|X_{kno}^{query}|}{|X^{query}|}$ after Oracle labeling, a is the variation amplitude and z is the triggering threshold. Notably, although the number of hyper-parameters increases, setting them becomes significantly easier, and they are less sensitive to dataset variations.

3.3. Detector and Target Classifier Training

Detector training. All labeled examples from the known classes and unknown classes are jointly used to train a detector with $C + 1$ classes. For a given data point x_i with label y_i , let p_i denote its one-hot label, i.e., p_{ic} is set to 1 and the others to 0, and q_i denote its probability vector predicted by the detector. On the one hand, we use the following cross-entropy loss to train the detector:

$$\mathcal{L}_{ce}^{x_i} = -p_i \log q_i = -\sum_{c=1}^{C+1} p_{ic} \log q_{ic}. \quad (11)$$

On the other hand, we propose a margin-based energy loss to ensure that, for examples from known classes, the free energy scores for the first C classes are high, while for examples from unknown classes, the free energy score for the $(C + 1)$ -th class remains low, referring to Remark 1. The energy loss is calculated by⁴:

$$\mathcal{L}_{energy}^{x_i} = \begin{cases} (\max(0, E_{kno}(x_i) - m_{kno}))^2 & \text{if } x_i \in \mathcal{D}_L^{kno}, \\ (\max(0, m_{unk} - E_{kno}(x_i)))^2 & \text{if } x_i \in \mathcal{D}_L^{unk}, \end{cases} \quad (12)$$

where m_{kno} and m_{unk} are the margins for known classes and unknown classes, respectively.

Thus, the total loss for training the detector is:

$$\mathcal{L}_{detector}^{x_i} = \mathcal{L}_{ce}^{x_i} + \lambda_e \mathcal{L}_{energy}^{x_i}, \quad (13)$$

where λ_e is a hyper-parameter that balances the two losses.

Target classifier training. All labeled examples from the known classes are used to train the target classifier by minimizing the standard cross-entropy loss:

$$\mathcal{L}_{classifier}^{x_i} = -p_i \log q_i = -\sum_{c=1}^C p_{ic} \log q_{ic}. \quad (14)$$

The pseudocode of EAOA is shown in Appendix C.

4. Experiments

4.1. Implementation Details

Datasets. We validate the effectiveness of our method on three benchmark datasets: CIFAR-10 [15], CIFAR-100

⁴Replacing $E_{kno}(x_i)$ with $EU(x_i)$ is also a suitable choice; however, we find that the performance difference between the two is minimal.

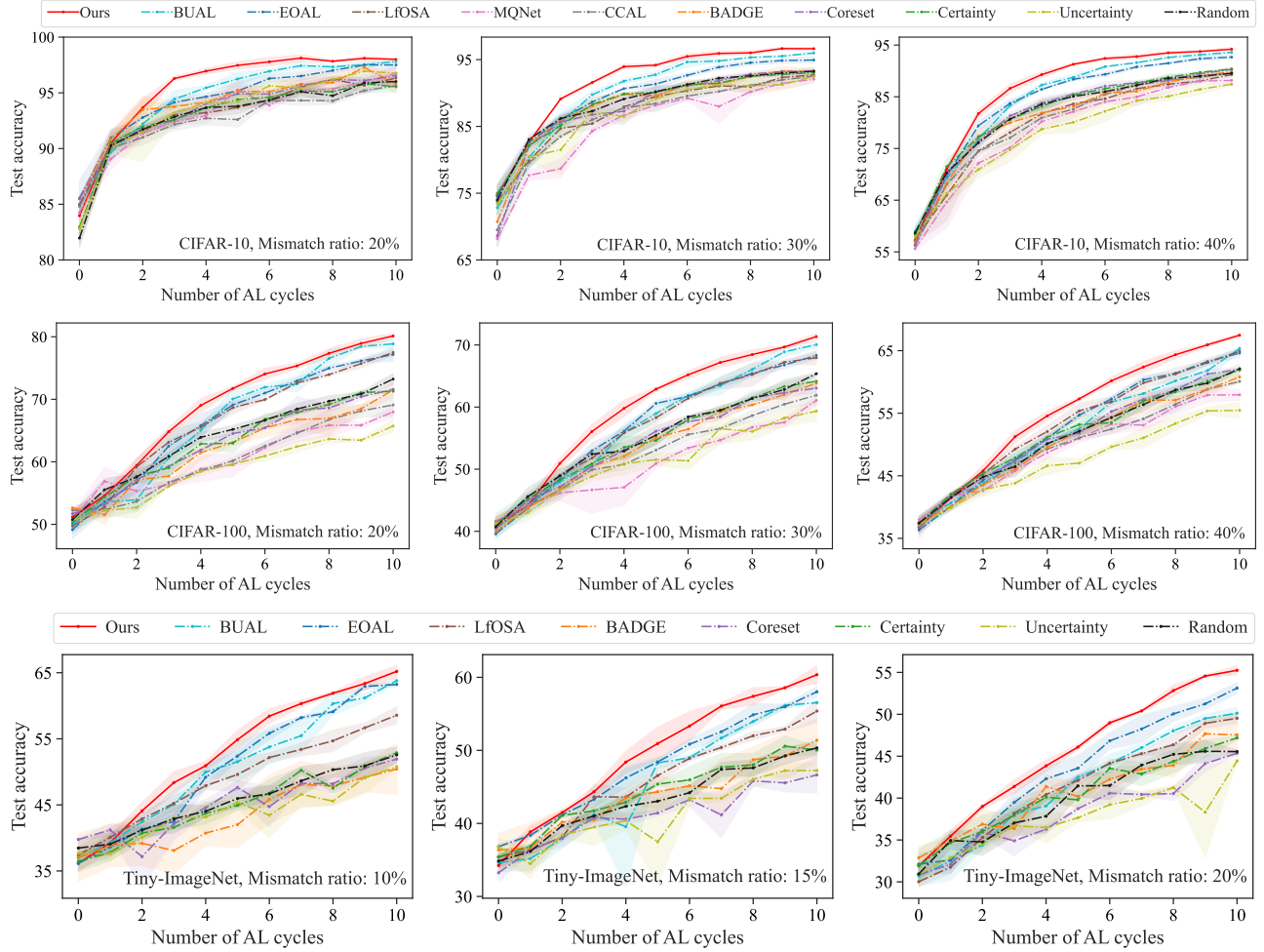


Figure 3. Test accuracy comparison on CIFAR-10, CIFAR-100, and Tiny-ImageNet.

[15], and Tiny-ImageNet [41], with category counts of 10, 100, and 200, respectively. To perform active open-set annotation (AOSA), we create their open-set versions by randomly selecting a subset of classes as known according to the specified mismatch ratio, while the remaining classes are treated as unknown. The mismatch ratio is defined as the proportion of known classes in the total number of classes. For CIFAR-10 and CIFAR-100, we set the mismatch ratios to 20%, 30%, and 40%. For Tiny-ImageNet, we set the ratios to 10%, 15%, and 20%, making it more challenging.

Training details. Initially, we randomly select 1%, 8%, and 8% of known class examples from CIFAR-10, CIFAR-100, and Tiny-ImageNet, respectively, to construct the labeled dataset. The active learning (AL) process consists of 10 rounds, with 1,500 examples queried in each round. For all experiments, we choose ResNet-18 [9] as the base model and train it by SGD [48] optimizer with momentum 0.9, weight decay $5e-4$, and batch size 128 for 200 epochs. The initial learning rate is set to 0.01 and is reduced by a fac-

tor of 10 every 60 epochs. We repeat all experiments three times on GeForce RTX 3090 GPUs and record the average results for three random seeds ($seed = 1, 2, 3$). We generally set the values of K , tP , k_1 , a , z , m_{kno} , m_{unk} , and λ_e to 250, 0.6, 5, 1, 0.05, -25, -7, and 0.01, respectively, and these values generalize well across datasets.

Baselines. We consider the following methods as baselines: Random, Uncertainty, Certainty, Coreset, BADGE, CCAL, MQNet, EOAL, and BUAL. Among them, EOAL and BUAL are currently state-of-the-art (SOTA). A detailed overview of these methods is provided in Appendix D.

4.2. Performance Comparison

Figure 3 displays the test accuracy of various methods on CIFAR-10, CIFAR-100, and Tiny-ImageNet, varying with the number of AL rounds. Figure 4 presents scatter plots of the average query precision across all rounds and the final round test accuracy for each method on CIFAR-10, CIFAR-100, and Tiny-ImageNet. Here, the query precision refers to

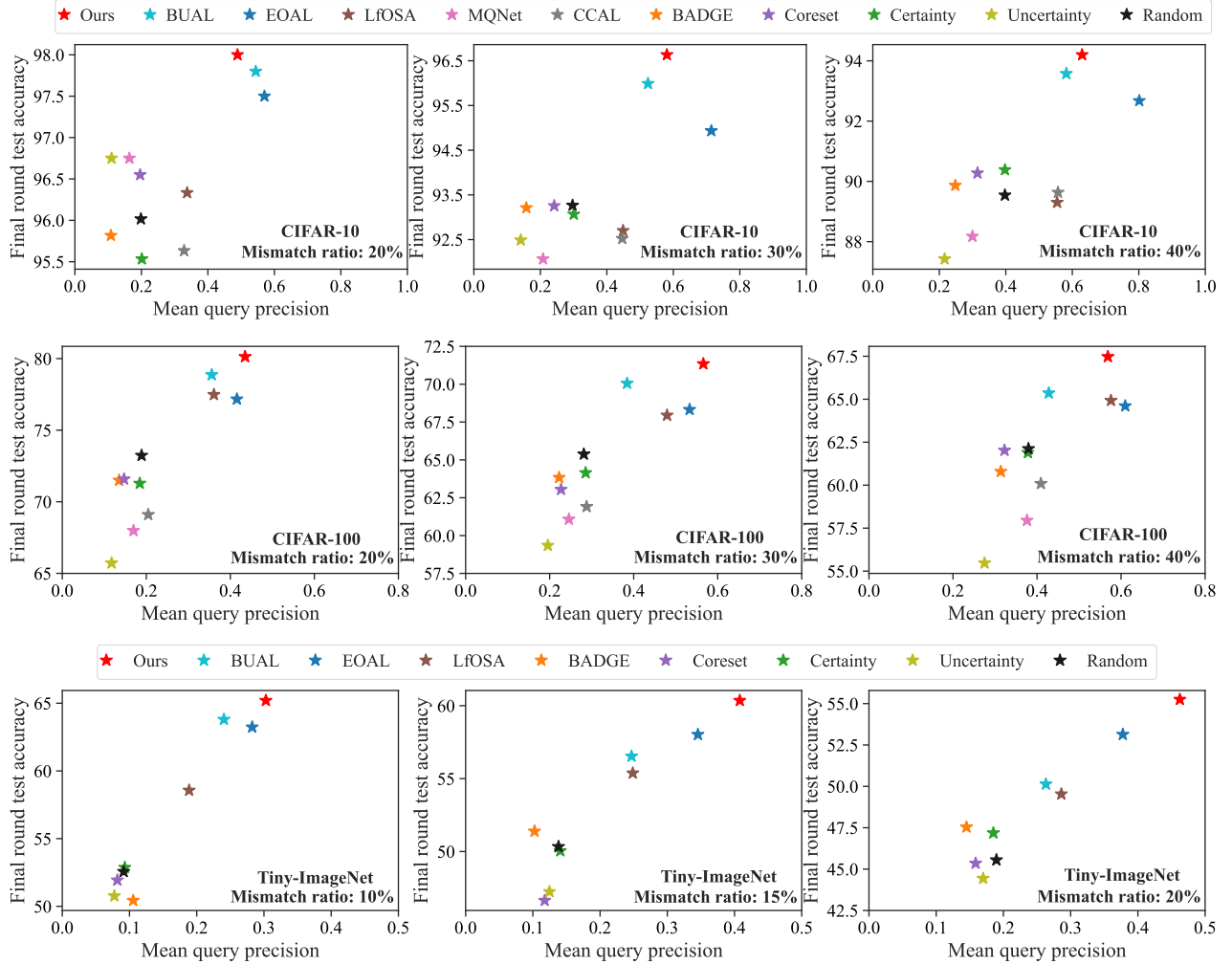


Figure 4. Query precision comparison on CIFAR-10, CIFAR-100, and Tiny-ImageNet.

the proportion of queried known class examples to the total number of queried examples in each round.

As shown in Figure 3, our method achieves optimal test accuracy across all datasets and mismatch ratios, and in most AL rounds, the curve of our method completely overlaps with those of other methods, demonstrating its superiority. In Figure 4, our method achieves optimal final round test accuracy and mean query precision in most scenarios, particularly on the challenging Tiny-ImageNet dataset, demonstrating its strong recognition capabilities. Compared to the existing SOTA methods, BUAL and EOAL, our method ensures that queried examples exhibit low epistemic uncertainty while maintaining high aleatoric uncertainty. The significant test performance improvement over them validates the effectiveness of our proposed framework, suggesting that the examples selected by our method are more informative. All methods that employ a $(C+1)$ -class detector to leverage labeled unknown class examples—BUAL,

EOAL, LfOSA, and our method—exhibit significant performance advantages over the remaining methods, both in test performance and recognition capability. Although CCAL and MQNet consider both sample purity and informativeness, they fail to achieve an effective balance and adopt inadequate measurement metrics. Certainty shows similar recognition performance to Random, supporting that entropy, i.e., a measure of aleatoric uncertainty, is only meaningful in closed-set scenarios. Traditional AL methods, Uncertainty, Coreset, and BADGE, are significantly hindered by open-set examples, as these examples are prone to receive low-confidence predictions and exhibit diverse features, thus leading to poorer performance.

4.3. Ablation Studies

Effect of each component. Figure 5 (left) shows the ablation results to validate the effectiveness of each component in our method. Our proposed energy-based epistemic

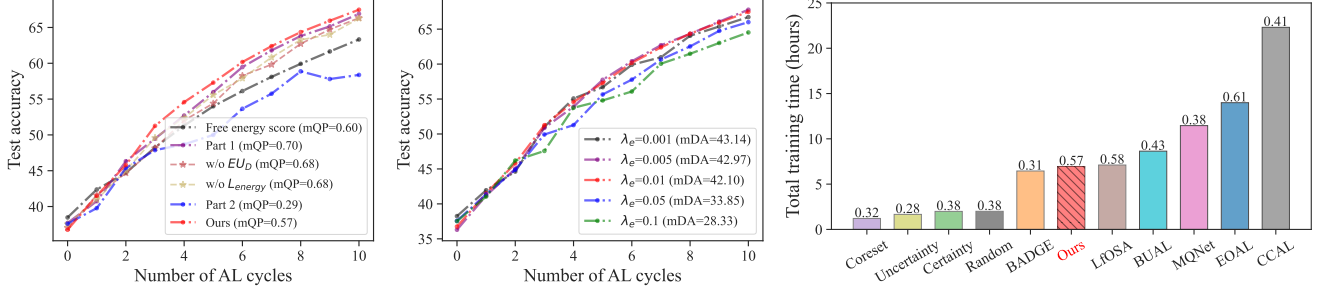


Figure 5. Ablation results on CIFAR-100 with a mismatch ratio of 40%. 1) The **left** validates the effectiveness of each method component. “Part 1” represents energy-based epistemic uncertainty and “Part 2” indicates energy-based aleatoric uncertainty. “mQP” denotes mean query precision across all AL rounds. 2) The **middle** assesses the sensitivity of the energy loss weight λ_e . “mDA” denotes mean detector test accuracy across all AL rounds. 3) The **right** shows the runtime comparison. The numbers on the bar chart correspond to mQP scores.

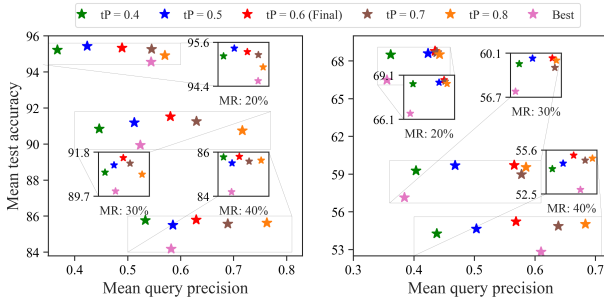


Figure 6. Ablation results for target precision tP on CIFAR-10 (**Left**) and CIFAR-100 (**Right**). “MR” denotes mismatch ratio. “Best” indicates the top-performing method in the comparisons.

uncertainty (“Part 1”) utilizes information from labeled unknown class examples, leading to significant improvements in both recognition and test performance compared to free energy alone. The proposed energy-based aleatoric uncertainty (“Part 2”) performs poorly on its own, as aleatoric uncertainty is only meaningful in closed-set scenarios. However, when combined with “Part 1”, it shows significant improvement, validating the superiority of the entire framework. Additionally, removing the data-driven epistemic uncertainty score or the margin-based energy loss leads to a decline in performance, confirming their necessity.

Hyper-parameter sensitivity. Figure 6 presents the ablation results for the hyperparameter target query precision tP on CIFAR-10 and CIFAR-100, with values set to [0.4, 0.5, 0.6, 0.7, 0.8]. Overall, the fluctuations in test performance are minimal, and as tP increases, the method’s recognition performance improves. Figure 5 (middle) displays the ablation results for the energy loss weight λ_e on CIFAR-100 with a 40% mismatch ratio, using values of [0.001, 0.005, 0.01, 0.05, 0.1]. A higher loss weight can impede model training, leading to reduced detector accuracy and reliability. Conversely, a lower loss weight fails to effectively separate the energy distributions of known and

unknown class examples, adversely affecting the detector’s recognition performance.

The ablation results for additional hyper-parameters are provided in Appendix E, which can demonstrate their ability to generalize effectively across different datasets.

Runtime comparison. Figure 5 (right) presents the running times and mean query precision of various methods on CIFAR-100 with a mismatch ratio of 40%. A higher mean query precision indicates that a larger number of examples are involved in training, often resulting in longer training times. Traditional AL methods, characterized by lower mean query precision and the training of a single model, generally have shorter training times. Notably, our method has the shortest runtime among all AOSA methods, achieving the highest test accuracy and maintaining a very high recognition rate.

5. Conclusion

In this paper, we demonstrate that focusing solely on either epistemic uncertainty (EU) or aleatoric uncertainty (AU) in open-world active learning scenarios does not yield satisfactory performance. We argue that the most informative examples should primarily belong to closed-set classes, exhibiting low EU scores, ensuring that the derived AU metric is meaningful, and secondarily, should show high AU scores. To achieve this, we propose EAOA, a novel framework for addressing the challenging active open-set annotation problem. In EAOA, both types of uncertainty are defined in the form of free energy: EU is evaluated by the detector from both learning-based and data-driven perspectives, while AU is measured by the target classifier through class confusion. Additionally, we introduce a margin-based energy loss to enhance the detector’s ability to distinguish known from unknown classes and a target-driven strategy to adaptively adjust the size of the candidate set obtained in the first query stage. Extensive experimental results across various tasks demonstrate EAOA’s superiority.

Acknowledgements

This work was supported by the Natural Science Foundation of Jiangsu Province of China (BK20222012) and the NSFC(U2441285, 62222605).

References

- [1] Jordan T Ash, Chicheng Zhang, Akshay Krishnamurthy, John Langford, and Alekh Agarwal. Deep batch active learning by diverse, uncertain gradient lower bounds. *arXiv preprint arXiv:1906.03671*, 2019. 1, 2
- [2] Maria-Florina Balcan, Andrei Broder, and Tong Zhang. Margin based active learning. In *International Conference on Computational Learning Theory*, pages 35–50. Springer, 2007. 1, 2
- [3] Abhijit Bendale and Terrance Boulton. Towards open world recognition. In *Proceedings of the IEEE conference on computer vision and pattern recognition*, pages 1893–1902, 2015. 2
- [4] Guangyao Chen, Limeng Qiao, Yemin Shi, Peixi Peng, Jia Li, Tiejun Huang, Shiliang Pu, and Yonghong Tian. Learning open set network with discriminative reciprocal points. In *Computer Vision–ECCV 2020: 16th European Conference, Glasgow, UK, August 23–28, 2020, Proceedings, Part III 16*, pages 507–522. Springer, 2020. 2
- [5] Guangyao Chen, Peixi Peng, Xiangqian Wang, and Yonghong Tian. Adversarial reciprocal points learning for open set recognition. *IEEE Transactions on Pattern Analysis and Machine Intelligence*, 44(11):8065–8081, 2021. 2
- [6] Pan Du, Suyun Zhao, Hui Chen, Shuwen Chai, Hong Chen, and Cuiping Li. Contrastive coding for active learning under class distribution mismatch. In *Proceedings of the IEEE/CVF International Conference on Computer Vision*, pages 8927–8936, 2021. 1, 2, 3
- [7] Meng Fang, Yuan Li, and Trevor Cohn. Learning how to active learn: A deep reinforcement learning approach. *arXiv preprint arXiv:1708.02383*, 2017. 2
- [8] ZongYuan Ge, Sergey Demyanov, Zetao Chen, and Rahil Garnavi. Generative openmax for multi-class open set classification. *arXiv preprint arXiv:1707.07418*, 2017. 2
- [9] Kaiming He, Xiangyu Zhang, Shaoqing Ren, and Jian Sun. Deep residual learning for image recognition. In *Proceedings of the IEEE conference on computer vision and pattern recognition*, pages 770–778, 2016. 6
- [10] Alex Holub, Pietro Perona, and Michael C Burl. Entropy-based active learning for object recognition. In *2008 IEEE Computer Society Conference on Computer Vision and Pattern Recognition Workshops*, pages 1–8. IEEE, 2008. 1, 2
- [11] Sheng-Jun Huang, Rong Jin, and Zhi-Hua Zhou. Active learning by querying informative and representative examples. *Advances in neural information processing systems*, 23, 2010. 1, 2
- [12] Sheng-Jun Huang, Chen-Chen Zong, Kun-Peng Ning, and Haibo Ye. Asynchronous active learning with distributed label querying. In *IJCAI*, pages 2570–2576, 2021. 1, 2
- [13] Lalit P Jain, Walter J Scheirer, and Terrance E Boulton. Multi-class open set recognition using probability of inclusion. In *Computer Vision–ECCV 2014: 13th European Conference, Zurich, Switzerland, September 6–12, 2014, Proceedings, Part III 13*, pages 393–409. Springer, 2014. 2
- [14] Alex Kendall and Yarin Gal. What uncertainties do we need in bayesian deep learning for computer vision? *Advances in neural information processing systems*, 30, 2017. 2
- [15] A Krizhevsky. Learning multiple layers of features from tiny images. *Master’s thesis, University of Tront*, 2009. 5, 6
- [16] Yann LeCun, Yoshua Bengio, and Geoffrey Hinton. Deep learning. *nature*, 521(7553):436–444, 2015. 1
- [17] Mingkun Li and Ishwar K Sethi. Confidence-based active learning. *IEEE transactions on pattern analysis and machine intelligence*, 28(8):1251–1261, 2006. 2
- [18] Weitang Liu, Xiaoyun Wang, John Owens, and Yixuan Li. Energy-based out-of-distribution detection. *Advances in neural information processing systems*, 33:21464–21475, 2020. 3
- [19] Dwarikanath Mahapatra, Behzad Bozorgtabar, Jean-Philippe Thiran, and Mauricio Reyes. Efficient active learning for image classification and segmentation using a sample selection and conditional generative adversarial network. In *International Conference on Medical Image Computing and Computer-Assisted Intervention*, pages 580–588. Springer, 2018. 2
- [20] Christoph Mayer and Radu Timofte. Adversarial sampling for active learning. In *Proceedings of the IEEE/CVF Winter Conference on Applications of Computer Vision*, pages 3071–3079, 2020. 2
- [21] Pedro R Mendes Júnior, Roberto M De Souza, Rafael de O Werneck, Bernardo V Stein, Daniel V Pazinato, Waldir R De Almeida, Otávio AB Penatti, Ricardo da S Torres, and Anderson Rocha. Nearest neighbors distance ratio open-set classifier. *Machine Learning*, 106(3):359–386, 2017. 2
- [22] Jishnu Mukhoti, Andreas Kirsch, Joost van Amersfoort, Philip HS Torr, and Yarin Gal. Deep deterministic uncertainty: A new simple baseline. In *Proceedings of the IEEE/CVF Conference on Computer Vision and Pattern Recognition*, pages 24384–24394, 2023. 2
- [23] Alexander Narr, Rudolph Triebel, and Daniel Cremers. Stream-based active learning for efficient and adaptive classification of 3d objects. In *2016 IEEE International Conference on Robotics and Automation (ICRA)*, pages 227–233. IEEE, 2016. 2
- [24] Lawrence Neal, Matthew Olson, Xiaoli Fern, Weng-Keen Wong, and Fuxin Li. Open set learning with counterfactual images. In *Proceedings of the European conference on computer vision (ECCV)*, pages 613–628, 2018. 2
- [25] Hieu T Nguyen and Arnold Smeulders. Active learning using pre-clustering. In *Proceedings of the twenty-first international conference on Machine learning*, page 79, 2004. 1, 2
- [26] Kun-Peng Ning, Xun Zhao, Yu Li, and Sheng-Jun Huang. Active learning for open-set annotation. In *Proceedings of the IEEE/CVF Conference on Computer Vision and Pattern Recognition*, pages 41–49, 2022. 1, 2, 3
- [27] Poojan Oza and Vishal M Patel. C2ae: Class conditioned auto-encoder for open-set recognition. In *Proceedings of*

- the *IEEE/CVF conference on computer vision and pattern recognition*, pages 2307–2316, 2019. 2
- [28] Dongmin Park, Yooju Shin, Jihwan Bang, Youngjun Lee, Hwanjun Song, and Jae-Gil Lee. Meta-query-net: Resolving purity-informativeness dilemma in open-set active learning. *Advances in Neural Information Processing Systems*, 35:31416–31429, 2022. 1, 2, 3
- [29] Pramuditha Perera, Vlad I Morariu, Rajiv Jain, Varun Manjunatha, Curtis Wigington, Vicente Ordonez, and Vishal M Patel. Generative-discriminative feature representations for open-set recognition. In *Proceedings of the IEEE/CVF conference on computer vision and pattern recognition*, pages 11814–11823, 2020. 2
- [30] Pengzhen Ren, Yun Xiao, Xiaojun Chang, Po-Yao Huang, Zhihui Li, Brij B Gupta, Xiaojiang Chen, and Xin Wang. A survey of deep active learning. *ACM computing surveys (CSUR)*, 54(9):1–40, 2021. 1
- [31] Bardia Safaei, VS Vibashan, Celso M de Melo, and Vishal M Patel. Entropic open-set active learning. In *Proceedings of the AAAI Conference on Artificial Intelligence*, pages 4686–4694, 2024. 1, 2, 3
- [32] Walter J Scheirer, Lalit P Jain, and Terrance E Boult. Probability models for open set recognition. *IEEE transactions on pattern analysis and machine intelligence*, 36(11):2317–2324, 2014. 2
- [33] Ozan Sener and Silvio Savarese. Active learning for convolutional neural networks: A core-set approach. *arXiv preprint arXiv:1708.00489*, 2017. 1, 2
- [34] Burr Settles. Active learning literature survey. *Computer Sciences Technical Report*, 2009. 1
- [35] Lewis Smith and Yarin Gal. Understanding measures of uncertainty for adversarial example detection. *arXiv preprint arXiv:1803.08533*, 2018. 2
- [36] Xin Sun, Zhenning Yang, Chi Zhang, Keck-Voon Ling, and Guohao Peng. Conditional gaussian distribution learning for open set recognition. In *Proceedings of the IEEE/CVF conference on computer vision and pattern recognition*, pages 13480–13489, 2020. 2
- [37] Jesper E Van Engelen and Holger H Hoos. A survey on semi-supervised learning. *Machine learning*, 109(2):373–440, 2020. 1
- [38] Sagar Vaze, Kai Han, Andrea Vedaldi, and Andrew Zisserman. Open-set recognition: a good closed-set classifier is all you need? *arXiv preprint arXiv:2110.06207*, 2021. 3
- [39] Haoran Wang, Weitang Liu, Alex Bocchieri, and Yixuan Li. Can multi-label classification networks know what they don’t know? *Advances in Neural Information Processing Systems*, 34:29074–29087, 2021. 3
- [40] Yichen Xie, Han Lu, Junchi Yan, Xiaokang Yang, Masayoshi Tomizuka, and Wei Zhan. Active finetuning: Exploiting annotation budget in the pretraining-finetuning paradigm. In *Proceedings of the IEEE/CVF Conference on Computer Vision and Pattern Recognition*, pages 23715–23724, 2023. 1, 2
- [41] Leon Yao and John Miller. Tiny imagenet classification with convolutional neural networks. *CS 231N*, 2(5):8, 2015. 6
- [42] Donggeun Yoo and In So Kweon. Learning loss for active learning. In *Proceedings of the IEEE/CVF conference on computer vision and pattern recognition*, pages 93–102, 2019. 1, 2
- [43] He Zhang and Vishal M Patel. Sparse representation-based open set recognition. *IEEE transactions on pattern analysis and machine intelligence*, 39(8):1690–1696, 2016. 2
- [44] Hongjie Zhang, Ang Li, Jie Guo, and Yanwen Guo. Hybrid models for open set recognition. In *Computer Vision–ECCV 2020: 16th European Conference, Glasgow, UK, August 23–28, 2020, Proceedings, Part III 16*, pages 102–117. Springer, 2020. 2
- [45] Da-Wei Zhou, Han-Jia Ye, and De-Chuan Zhan. Learning placeholders for open-set recognition. In *Proceedings of the IEEE/CVF conference on computer vision and pattern recognition*, pages 4401–4410, 2021. 2
- [46] Zhi-Hua Zhou. A brief introduction to weakly supervised learning. *National science review*, 5(1):44–53, 2018. 1
- [47] Jia-Jie Zhu and José Bento. Generative adversarial active learning. *arXiv preprint arXiv:1702.07956*, 2017. 2
- [48] Martin Zinkevich, Markus Weimer, Lihong Li, and Alex Smola. Parallelized stochastic gradient descent. *Advances in neural information processing systems*, 23, 2010. 6
- [49] Chen-Chen Zong, Ye-Wen Wang, Ming-Kun Xie, and Sheng-Jun Huang. Dirichlet-based prediction calibration for learning with noisy labels. In *Proceedings of the AAAI Conference on Artificial Intelligence*, pages 17254–17262, 2024. 1
- [50] Chen-Chen Zong, Ye-Wen Wang, Kun-Peng Ning, Hai-Bo Ye, and Sheng-Jun Huang. Bidirectional uncertainty-based active learning for open-set annotation. In *Computer Vision – ECCV 2024*, pages 127–143, Cham, 2025. Springer Nature Switzerland. 1, 2, 3

Rethinking Epistemic and Aleatoric Uncertainty for Active Open-Set Annotation: An Energy-Based Approach

Supplementary Material

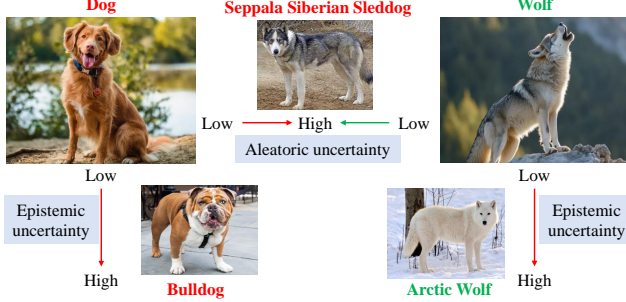


Figure 7. Intuitive examples of aleatoric and epistemic uncertainty in dog-wolf binary classification.

A. Uncertainty Quantification

In deep learning, epistemic uncertainty and aleatoric uncertainty represent two distinct types of uncertainty, commonly used to describe the various sources of uncertainty in a model’s predictions:

- **Epistemic uncertainty:**
 - This type of uncertainty arises from a model’s lack of knowledge, often due to insufficient training data or the model’s complexity. It reflects the model’s incomplete or uncertain understanding of the task and can generally be reduced or eliminated with more data or a more effective model.
 - For example, in a deep neural network, if there is little data available for certain classes or the model has not been trained sufficiently, the model may be highly uncertain in its predictions for certain examples.
 - This uncertainty is generally reducible, as it can be mitigated by adding more training data or improving the model architecture.
 - In Figure 7, the “Bulldog” and “Arctic Wolf” exhibit significant feature differences from the “Dog” and “Wolf” in the training set, leading to higher epistemic uncertainty. After these examples are incorporated into model training, predictive performance on them improves, thereby reducing their epistemic uncertainty.
- **Aleatoric uncertainty:**
 - This type of uncertainty stems from inherent noise or variability in the data, i.e., the intrinsic randomness or uncontrollable factors within the data.
 - For instance, in image classification, factors like feature confusion, lighting conditions, or object occlusion may lead to instability in the model’s predictions.
 - This uncertainty is generally irreducible because it

originates from the intrinsic properties of the data, not from issues with the model or training process.

- In Figure 7, the “Seppala Siberian Sleddog” resembles the “Wolf” in appearance but belongs to the “Dog” class, leading to higher aleatoric uncertainty. Due to feature confusion, incorporating these examples into model training may not substantially improve performance or reduce their aleatoric uncertainty.

B. Label-Wise Free Energy

EBMs define the probability distribution in multi-label settings through the logits as:

$$\begin{aligned}
 p(y_c|x) &= \frac{e^{-E(x,y_c)}}{\int_y e^{-E(x,y_c)}} = \frac{e^{-E(x,y_c)}}{e^{-E(x,y_c)} + e^{-E(x,-y_c)}} \\
 &= \frac{e^{-E(x,y_c)+E(x,-y_c)}}{1 + e^{-E(x,y_c)+E(x,-y_c)}} = \frac{e^{f_{y_c}(x)}}{1 + e^{f_{y_c}(x)}} \quad (15) \\
 &= \frac{e^{-E(x,y_c)}}{e^{-E(x)}}
 \end{aligned}$$

where $y_c = 1$ indicates that instance x belongs to the c -th class while $y_c = -1$ indicates not, $f_{y_c}(x)$ denotes predicted logit of the model f for instance x regarding the c -th class, and $E_{y_c}(x) = -\log(1 + e^{f_{y_c}(x)})$ is the label-wise free energy for instance x on class y_c .

C. The Pseudocode of EAOA

The pseudocode of EAOA is summarized in Algorithm 1.

D. Comparing Methods

We consider the following AL methods as baselines:

- Random, which selects instances at random;
- Uncertainty, which selects instances with the highest entropy of predictions;
- Certainty, which selects instances with the lowest entropy of predictions;
- Coreset, which uses the concept of core-set selection to choose diverse instances;
- BADGE, which selects instances by considering both uncertainty and diversity in the gradient via k-means++ clustering;
- CCAL, which employs contrastive learning to extract the semantic and distinctive scores of examples for instance querying;
- MQNet, which balances the purity score and informativeness score to select instances through meta-learning;

Algorithm 1 The EAOA algorithm

Input: Labeled data pool $\mathcal{D}_L = \mathcal{D}_L^{kno} \cup \mathcal{D}_L^{unk}$, unlabeled data pool \mathcal{D}_U , detector f_{θ_D} , target classifier f_{θ_C} , query budget b , dynamic factor k_t , and target precision tP .

Process: (The t -th AL round)

- 1: # Detector training
- 2: Update θ_D by minimizing $\mathcal{L}_{detector}$ in Eq. (13) using all labeled examples from \mathcal{D}_L .
- 3: # Epistemic uncertainty estimating
- 4: Extract logit outputs and features from f_{θ_D} for examples in \mathcal{D}_L and \mathcal{D}_U , respectively.
- 5: Based on model outputs, estimate the learning-based epistemic uncertainty score for each example in \mathcal{D}_U using Eq. (1) and Remark 1.
- 6: Based on feature similarity, find K -nearest neighbors in \mathcal{D}_U for each example in \mathcal{D}_L , and obtain reverse neighbors by class in \mathcal{D}_L for each example in \mathcal{D}_U .
- 7: Estimate data-centric epistemic uncertainty score for each example in \mathcal{D}_U using Eq. (7) and Remark 1.
- 8: For each example, combine the two scores into one final epistemic uncertainty score using GMM and Eq. (8).
- 9: # Target classifier training
- 10: Update θ_C by minimizing $\mathcal{L}_{classifier}$ in Eq. (14) using all known class labeled examples from \mathcal{D}_L^{kno} .
- 11: # Aleatoric uncertainty estimating
- 12: Extract logit outputs from f_{θ_C} for examples in \mathcal{D}_U .
- 13: Estimate aleatoric uncertainty score for each example in \mathcal{D}_U using Remark 2.
- 14: # Active sampling
- 15: $k_t b$ examples with the lowest epistemic uncertainty scores are selected first to form a candidate query set.
- 16: b examples with the highest aleatoric uncertainty scores are then queried to form the final query set X^{query} .
- 17: # Oracle labeling
- 18: Query labels from Oracle and obtain X_{kno}^{query} , X_{unk}^{query} , and query precision $rP = \frac{|X_{kno}^{query}|}{|X^{query}|}$.
- 19: Update k_t to k_{t+1} using Eq. (10) based on $tP - rP$.
- 20: Update corresponding data pools: $\mathcal{D}_U = \mathcal{D}_U - X^{query}$, $\mathcal{D}_L^{kno} = \mathcal{D}_L^{kno} \cup X_{kno}^{query}$, and $\mathcal{D}_L^{unk} = \mathcal{D}_L^{unk} \cup X_{unk}^{query}$.

Output: \mathcal{D}_L , \mathcal{D}_U , θ_D , θ_C , and k_{t+1} for next round.

- LfOSA, which selects instances based on the maximum activation value produced by the $(C + 1)$ -class detector;
- EOAL, which queries instances by calculating the entropy of examples in both known and unknown classes;
- BUAL, which queries instances by adaptively combining the uncertainty obtained from positive and negative classifiers trained in different ways.

Among these methods, EOAL and BUAL are currently state-of-the-art.

E. Additional Ablation Studies

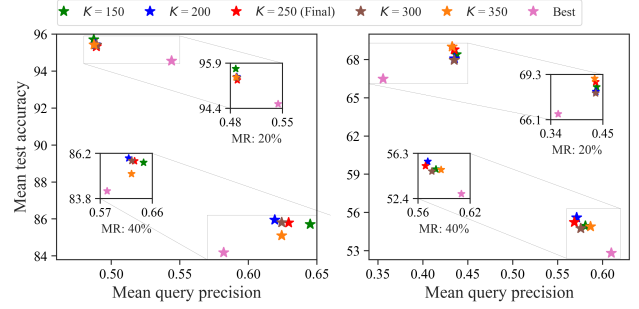


Figure 8. Ablation results for K in reverse k-NN on CIFAR-10 (Left) and CIFAR-100 (Right). “MR” denotes mismatch ratio. “Best” indicates the top-performing method in the comparisons.

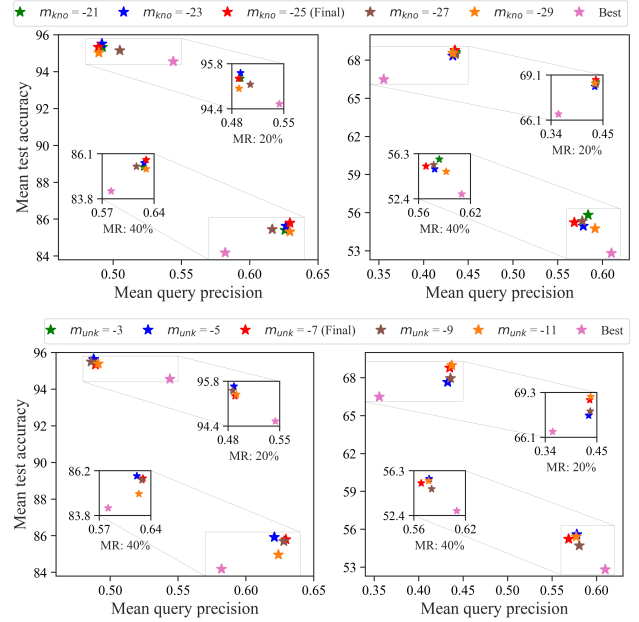


Figure 9. Ablation results for m_{kno} and m_{unk} in margin-based energy loss on CIFAR-10 (Left) and CIFAR-100 (Right).

Figure 8 illustrates the effect of the hyperparameter K in reverse k-NN on EAOA’s performance, with values set to [150, 200, 250, 300, 350]. Figure 9 presents the influence of the known class margin m_{kno} and the unknown class margin m_{unk} in margin-based energy loss \mathcal{L}_{energy} on EAOA’s performance, with values set to [-29, -27, -25, -23, -21] for m_{kno} and [-11, -9, -7, -5, -3] for m_{unk} . While the optimal value of K , m_{kno} , and m_{unk} differ across different settings, their overall performance remains relatively stable compared to the top-performing method in the comparisons, with $K = 250$, $m_{kno} = -25$, and $m_{unk} = -7$ consistently achieving strong results.

